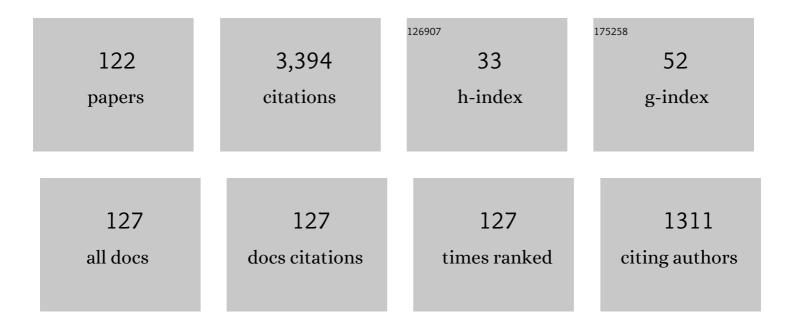
Li-Juan Chen

List of Publications by Year in descending order

Source: https://exaly.com/author-pdf/427964/publications.pdf Version: 2024-02-01



#	Article	IF	CITATIONS
1	Research progress on polyoxometalate-based transition-metal–rare-earth heterometallic derived materials: synthetic strategies, structural overview and functional applications. Chemical Communications, 2016, 52, 4418-4445.	4.1	245
2	Aggregation of Giant Cerium–Bismuth Tungstate Clusters into a 3D Porous Framework with High Proton Conductivity. Angewandte Chemie - International Edition, 2018, 57, 8416-8420.	13.8	221
3	Multicomponent Selfâ€Assembly of a Giant Heterometallic Polyoxotungstate Supercluster with Antitumor Activity. Angewandte Chemie - International Edition, 2021, 60, 11153-11157.	13.8	145
4	Polyoxometalate-based composite materials in electrochemistry: state-of-the-art progress and future outlook. Nanoscale, 2020, 12, 5705-5718.	5.6	118
5	Structural Transformation from Dimerization to Tetramerization of Serineâ€Decorated Rareâ€Earthâ€Incorporated Arsenotungstates Induced by the Usage of Rareâ€Earth Salts. Chemistry - A European Journal, 2017, 23, 2673-2689.	3.3	95
6	Significant developments in rare-earth-containing polyoxometalate chemistry: synthetic strategies, structural diversities and correlative properties. CrystEngComm, 2015, 17, 8175-8197.	2.6	77
7	A Series of Inorganicâ^'Organic Hybrid Composite Solids Based on Molybdenum Oxide Chains. Crystal Growth and Design, 2006, 6, 2076-2085.	3.0	71
8	Novel polyoxometalate hybrids consisting of copper–lanthanide heterometallic/lanthanide germanotungstate fragments. Dalton Transactions, 2012, 41, 10740.	3.3	71
9	Three Transition-Metal Substituted Polyoxotungstates Containing Keggin Fragments: From Trimer to One-Dimensional Chain to Two-Dimensional Sheet. Crystal Growth and Design, 2011, 11, 1913-1923.	3.0	68
10	First Tungstoantimonate-Based Transition-Metal–Lanthanide Heterometallic Hybrids Functionalized by Amino Acid Ligands. Crystal Growth and Design, 2014, 14, 6217-6229.	3.0	66
11	Trigonal Pyramidal {AsO ₂ (OH)} Bridging Tetranuclear Rare-Earth Encapsulated Polyoxotungstate Aggregates. Inorganic Chemistry, 2016, 55, 3881-3893.	4.0	63
12	Four types of 1D or 2D organic–inorganic hybrids assembled by arsenotungstates and Cull–LnIII/IV heterometals. CrystEngComm, 2012, 14, 3108.	2.6	58
13	Syntheses, structures and electrochemical properties of a class of 1-D double chain polyoxotungstate hybrids [H ₂ dap][Cu(dap) ₂] _{0.5} [Cu(dap) ₂ (H ₂ O)][Ln(H< Dalton Transactions, 2014, 43, 5694-5706.	sub>2 <td>ub⁵³O)<sub< td=""></sub<></td>	ub ⁵³ O) <sub< td=""></sub<>
14	Tellurotungstate-Based Organotin–Rare-Earth Heterometallic Hybrids with Four Organic Components. Inorganic Chemistry, 2017, 56, 7257-7269.	4.0	53
15	Two organic–inorganic hybrid 1-D and 3-D polyoxotungstates constructed from hexa-Cull substituted sandwich-type arsenotungstate units. CrystEngComm, 2012, 14, 2797.	2.6	52
16	Two 1-D multi-nickel substituted arsenotungstate aggregates. CrystEngComm, 2011, 13, 3462.	2.6	51
17	Two novel 2D organic–inorganic hybrid lacunary Keggin phosphotungstate 3d–4f heterometallic derivatives: [Cu(en)2]2H6[Ce(α-PW11O39)2]·8H2O and [Cu(dap)2(H2O)][Cu(dap)2]4.5[Dy(α-PW11O39)2]Â Inorganic Chemistry Communication, 2011, 14, 324-329.	• \$H 92O.	50
18	Synergistic Effect between Different Coordination Geometries of Lanthanides and Various Coordination Modes of 2-Picolinic Acid Ligands Tuning Three Types of Rare 3d–4f Heterometallic Tungstoantimonates. Inorganic Chemistry, 2018, 57, 15079-15092.	4.0	50

#	Article	lF	CITATIONS
19	A brief review of the crucial progress on heterometallic polyoxotungstates in the past decade. CrystEngComm, 2016, 18, 842-862.	2.6	47
20	Two types of novel tetra-iron substituted sandwich-type arsenotungastates with supporting lanthanide pendants. Dalton Transactions, 2015, 44, 12598-12612.	3.3	46
21	Novel One-Dimensional Organic–Inorganic Polyoxometalate Hybrids Constructed from Heteropolymolybdate Units and Copper–Aminoacid Complexes. Crystal Growth and Design, 2014, 14, 1467-1475.	3.0	45
22	The main progress over the past decade and future outlook on high-nuclear transition-metal substituted polyoxotungstates: from synthetic strategies, structural features to functional properties. Dalton Transactions, 2016, 45, 4935-4960.	3.3	45
23	Double-Oxalate-Bridging Tetralanthanide Containing Divacant Lindqvist Isopolytungstates with an Energy Transfer Mechanism and Luminous Color Adjustablility Through Eu ³⁺ /Tb ³⁺ Codoping. Inorganic Chemistry, 2020, 59, 648-660.	4.0	44
24	An unprecedented dumbbell-shaped pentadeca-nuclear W-Er heterometal cluster stabilizing nanoscale hexameric arsenotungstate aggregate and electrochemical sensing properties of its conductive hybrid film-modified electrode. Nano Research, 2022, 15, 3628-3637.	10.4	40
25	Novel 1-D double-chain organic–inorganic hybrid polyoxotungstates constructed from dimeric copper–lanthanide heterometallic silicotungstate units. CrystEngComm, 2012, 14, 7981.	2.6	38
26	Tetrahedral Polyoxometalate Nanoclusters with Tetrameric Rare-Earth Cores and Germanotungstate Vertexes. Crystal Growth and Design, 2013, 13, 4368-4377.	3.0	38
27	Lanthanide-Connecting and Lone-Electron-Pair Active Trigonal-Pyramidal-AsO3 Inducing Nanosized Poly(polyoxotungstate) Aggregates and Their Anticancer Activities. Scientific Reports, 2016, 6, 26406.	3.3	37
28	Coexistence of long-range ferromagnetic ordering and spin-glass behavior observed in the first inorganic–organic hybrid 1-D oxalate-bridging nona-Mn ^{II} sandwiched tungstoantimonate chain. Journal of Materials Chemistry C, 2017, 5, 2043-2055.	5.5	37
29	Two Ce ³⁺ -Substituted Selenotungstates Regulated by <i>N</i> , <i>N</i> -Dimethylethanolamine and Dimethylamine Hydrochloride. Inorganic Chemistry, 2019, 58, 8442-8450.	4.0	37
30	Rectangle versus Square Oxalate-Connective Tetralanthanide Cluster Anchored in Lacunary Lindqvist Isopolytungstates: Syntheses, Structures, and Properties. Crystal Growth and Design, 2014, 14, 5495-5505.	3.0	35
31	Rare-Earth-Incorporated Tellurotungstate Hybrids Functionalized by 2-Picolinic Acid Ligands: Syntheses, Structures, and Properties. Inorganic Chemistry, 2017, 56, 13228-13240.	4.0	35
32	Hexameric to Trimeric Lanthanide-Included Selenotungstates and Their 2D Honeycomb Organic–Inorganic Hybrid Films Used for Detecting Ochratoxin A. ACS Applied Materials & Interfaces, 2021, 13, 35997-36010.	8.0	35
33	Rare-Earth and Antimony-Oxo Clusters Simultaneously Connecting Antimonotungstates Comprising Divacant and Tetravacant Keggin Fragments. Inorganic Chemistry, 2019, 58, 11636-11648.	4.0	33
34	The first purely inorganic polyoxotungstates constructed from dimeric tungstoantimonate-based iron–rare-earth heterometallic fragments. CrystEngComm, 2015, 17, 5002-5013.	2.6	32
35	Three Types of Distinguishing <scp>l</scp> -Alanine-Decorated and Rare-Earth-Incorporated Arsenotungstate Hybrids Prepared in a Facile One-Step Assembly Strategy. Inorganic Chemistry, 2019, 58, 3479-3491.	4.0	32
36	One-pot syntheses, structures and properties of two novel 1-D copper complexes: [Cull2(Hbpdc)2Cl2]2·2H2O and Cul(H2bpdc)Cl (H2bpdc = 2,2′-bipyridyl-5,5′-dicarboxylic acid). Inorganic Chemistry Communication, 2010, 13, 822-827.	3.9	30

#	Article	IF	CITATIONS
37	First Dimethyltin-Functionalized Rare-Earth Incorporated Tellurotungstates Consisting of {B·Î±-TeW ₇ O ₂₈ } and {W ₅ O ₁₈ } Mixed Building Units. Inorganic Chemistry, 2018, 57, 12509-12520.	4.0	30
38	Aggregation of Giant Cerium–Bismuth Tungstate Clusters into a 3D Porous Framework with High Proton Conductivity. Angewandte Chemie, 2018, 130, 8552-8556.	2.0	30
39	Organic–Inorganic Hybrid Cerium-Encapsulated Selenotungstate Including Three Building Blocks and Its Electrochemical Detection of Dopamine and Paracetamol. Inorganic Chemistry, 2020, 59, 15355-15364.	4.0	30
40	Acetate-Decorated Tri-Ln(III)-Containing Antimonotungstates with a Tetrahedral {WO ₄ } Group as a Structure-Directing Template and Their Luminescence Properties. Inorganic Chemistry, 2020, 59, 3954-3963.	4.0	30
41	Organocounterions-Assisted and pH-Controlled Self-Assembly of Five Nanoscale High-Nuclear Lanthanide Substituted Heteropolytungstates. Crystal Growth and Design, 2017, 17, 3917-3928.	3.0	29
42	Synthesis, structure and magnetism of a 2-D organic–inorganic hybrid tetra-Coll-substituted sandwich-type Keggin germanotungstate: {[Co(dap)2(H2O)]2[Co(dap)2]2[Co4(Hdap)2(B-α-HGeW9O34)2]}Â-7H2O. Inorganic Chemistry Communication, 2011, 14, 1052-1056.	3.9	28
43	Multi-praseodymium-and-tungsten bridging octameric tellurotungstate and its 2D honeycomb composite film for detecting estrogen. Nanoscale, 2020, 12, 10842-10853.	5.6	28
44	An organic–inorganic hybrid nickel-substituted arsenotungstate consisting of three types of polyoxotungstate units. Inorganic Chemistry Communication, 2010, 13, 50-53.	3.9	26
45	Two unusual nanosized Nd ³⁺ -substituted selenotungstate aggregates simultaneously comprising lacunary Keggin and Dawson polyoxotungstate segments. Nanoscale, 2020, 12, 16091-16101.	5.6	26
46	Two Penta-RE ^{III} Encapsulated Tetravacant Dawson Selenotungstates and Nanoscale Derivatives and Their Luminescence Properties. Inorganic Chemistry, 2019, 58, 7078-7090.	4.0	25
47	Construction of Ln ³⁺ -Substituted Arsenotungstates Modified by 2,5-Thiophenedicarboxylic Acid and Application in Selective Fluorescence Detection of Ba ²⁺ in Aqueous Solution. Inorganic Chemistry, 2020, 59, 6839-6848.	4.0	25
48	Two 3d–4f heterometallic monovacant Keggin phosphotungstate derivatives. Journal of Coordination Chemistry, 2011, 64, 400-412.	2.2	24
49	2-D and 3-D phosphotungstate-based TM–Ln heterometallic derivatives constructed from dimeric [Ln(α-PW11O39)2]11â~ fragments and copper-organic complex linkers. Journal of Solid State Chemistry, 2012, 196, 29-39.	2.9	24
50	Self-Assembly of a Family of Isopolytungstates Induced by the Synergistic Effect of the Nature of Lanthanoids and the pH Variation in the Reaction Process: Syntheses, Structures, and Properties. Crystal Growth and Design, 2016, 16, 108-120.	3.0	24
51	An unprecedented polyhydroxycarboxylic acid ligand bridged multi-Eu ^{III} incorporated tellurotungstate and its luminescence properties. Dalton Transactions, 2020, 49, 8933-8948.	3.3	24
52	First quadruple-glycine bridging mono-lanthanide-substituted borotungstate hybrids. Dalton Transactions, 2016, 45, 16471-16484.	3.3	23
53	First series of mixed (P ^{III} , Se ^{IV})-heteroatomoriented rare-earth-embedded polyoxotungstates containing distinct building blocks. Inorganic Chemistry Frontiers, 2020, 7, 4640-4651.	6.0	23
54	A CdSO4-like 3-D framework constructed from monosodium substituted Keggin arsenotungstates and copper(II)-ethylenediamine complexes. Inorganic Chemistry Communication, 2009, 12, 707-710.	3.9	22

#	Article	IF	CITATIONS
55	Two Families of Rare-Earth-Substituted Dawson-type Monomeric and Dimeric Phosphotungstates Functionalized by Carboxylic Ligands. Crystal Growth and Design, 2017, 17, 5295-5308.	3.0	22
56	{HPO ₃ } and {WO ₄ } Simultaneously Induce the Assembly of Tri-Ln(III)-Incorporated Antimonotungstates and Their Photoluminescence Behaviors. Inorganic Chemistry, 2021, 60, 1037-1044.	4.0	22
57	Three 3D organic–inorganic hybrid heterometallic polyoxotungstates assembled from 1:2-type [Ln(α-SiW11O39)2]13┠silicotungstates and [Cu(dap)2]2+ linkers. Synthetic Metals, 2012, 162, 1558-1565.	3.9	21
58	Synthesis, structure and magnetism of a S-shaped multi-iron substituted arsenotungstate containing a trivacant Keggin [B-α-AsVW9O34]9┠and a hexavacant Keggin [α-AsVW6O26]11┠fragments. Journal of Solid State Chemistry, 2011, 184, 2756-2761.	2.9	20
59	A novel Dawson-like cerium(IV)-hybridizing selenotungstate Na13H7[Ce(SeW17O59)2]·31H2O. Inorganic Chemistry Communication, 2015, 56, 35-40.	3.9	19
60	Synthesis, structure and electrochemical properties of a Fe III –Ce III heterometallic sandwich-type tungstoantimonate with novel 2-D infinite structure [Ce(H 2 O) 8][Ce(H 2 O) 6][Fe 4 (H 2 O) 10 (B-β-SbW) Tj E	F@.q0001	rg B JT /Overlo
61	Tricarboxylic-Ligand-Decorated Lanthanoid-Inserted Heteropolyoxometalates Built by Mixed-Heteroatom-Directing Polyoxotungstate Units: Syntheses, Structures, and Electrochemical Sensing for 17β-Estradiol. Inorganic Chemistry, 2021, 60, 7536-7544.	4.0	19
62	An organic–inorganic hybrid 1-D double-chain copper–yttrium heterometallic silicotungstate [Cu(dap)2(H2O)]2{Cu(dap)2[α-H2SiW11O39Y(H2O)2]2}·10H2O. Inorganic Chemistry Communication, 2013, 27, 13-17.	3.9	17
63	Multi-Nuclear Rare-Earth-Implanted Tartaric Acid-Functionalized Selenotungstates and Their Fluorescent and Magnetic Properties. Inorganic Chemistry, 2021, 60, 2533-2541.	4.0	17
64	Unprecedented Selenium and Lanthanide Simultaneously Bridging Selenotungstate Aggregates Stabilized by Four Tetraâ€øacant Dawsonâ€like {Se ₂ W ₁₄ } Units. Chemistry - an Asian Journal, 2018, 13, 2897-2907.	3.3	16
65	Syntheses, structural characterization and photophysical properties of two series of rare-earth-isonicotinic-acid containing Waugh-type manganomolybdates. CrystEngComm, 2017, 19, 834-852.	2.6	15
66	Organic–inorganic hybrid 1-D double chain heteropolymolybdates constructed from plenary Keggin germanomolybdate anions and hepta-nuclear Cu–RE–pic heterometallic clusters. Dalton Transactions, 2019, 48, 15977-15988.	3.3	15
67	3-D Antimonotungstate Framework Based on 2,6-H ₂ pdca-connecting Iron–Cerium Heterometallic Krebs-type Polyoxotungstates for Detecting Small Biomolecules. Inorganic Chemistry, 2021, 60, 2663-2671.	4.0	15
68	Dual-heteroatom-templated lanthanoid-inserted heteropolyoxotungstates simultaneously comprising Dawson and Keggin subunits and their composite film applied for electrochemical immunosensing of auximone. Inorganic Chemistry Frontiers, 2022, 9, 350-362.	6.0	15
69	An organic–inorganic hybrid dimeric arsenotungstate [enH2]4{[Cu(en)2][(A-β-H2AsW9O34)Cu(en)2]2}·8H2O established by two trivacant Keggin [A-β-AsW9O34]9â^' fragments in the opposite orientation. Inorganic Chemistry Communication, 2011, 14, 1178-1182.	3.9	14
70	An organic–inorganic hybrid hexa-nickel substituted sandwich-type germanotungstate [enH2]2[Ni(en)2]2{[Ni6(en)2(H2O)2][B-α-GeW9O34]2} 14H2O. Inorganic Chemistry Communication, 2012, 17, 79-83.	3.9	14
71	Syntheses, structures, spectroscopic and electrochemical properties of two 1D organic–inorganic Cull–LnIII heterometallic germanotungstates. Spectrochimica Acta - Part A: Molecular and Biomolecular Spectroscopy, 2013, 114, 360-367.	3.9	14
72	Recent progress in metal-functionalized germanotungstates: from structures to properties. RSC Advances, 2014, 4, 50679-50692.	3.6	13

#	Article	IF	CITATIONS
73	Syntheses, structures and fluorescence properties of three rare-earth containing docosatungstates. Spectrochimica Acta - Part A: Molecular and Biomolecular Spectroscopy, 2017, 176, 114-122.	3.9	13
74	Ligandâ€Controlled Assembly of Heteropolyoxomolybdates from Plenary Keggin Germanomolybdates and Cu–Ln Heterometallic Units. Chemistry - an Asian Journal, 2018, 13, 3762-3775.	3.3	13
75	Three Lanthanide-Functionalized Antimonotungstate Clusters with a {Sb ₄ O ₄ Ln ₃ (H ₂ O) ₈ } Core: Syntheses, Structures, and Properties. Inorganic Chemistry, 2021, 60, 18065-18074.	4.0	13
76	Hydrothermal syntheses and structural characterization of two sandwich-type arsenotungstates. Journal of Coordination Chemistry, 2010, 63, 2042-2055.	2.2	12
77	Three novel 2D organic–inorganic hybrid Cull–LnIII heterometallic arsenotungstates. Synthetic Metals, 2012, 162, 1030-1036.	3.9	12
78	2-Picolinate-Decorated Iron–Lanthanide Heterometallic Germanotungstates Including an S-Shaped [Ge ₂ W ₂₀ O ₇₂] ^{16–} Segment. Inorganic Chemistry, 2019, 58, 15853-15863.	4.0	12
79	Organic–Inorganic Two-Dimensional Hybrid Networks Constructed from Pyridine-4-Carboxylate-Decorated Organotin–Lanthanide Heterometallic Antimotungstates. Inorganic Chemistry, 2020, 59, 11287-11297.	4.0	12
80	A 2-D Organic–Inorganic Hybrid Copper-Yttrium Heterometallic Monovacant Keggin Phosphotungstate Derivative: [Cu(dap)2]5.5[Y(ĺ±-PW11O39)2]·4H2O. Synthesis and Reactivity in Inorganic, Metal Organic, and Nano Metal Chemistry, 2012, 42, 30-36.	0.6	11
81	Synthesis, structure and properties of a metal–organic complex built up from ferrous sulfate chains and 2,2'-bipyridyl-5,5'-dicarboxylic acid ligands. Inorganic Chemistry Communication, 2012, 20, 277-281.	3.9	11
82	A novel organic–inorganic hybrid sandwich-type germanotungstate with discrete [Fe4(en)2(l±-GeW9O34)2]8âî' polyoxoanions and 1-D [Fe4(en)(l±-GeW9O34)2]n8nâî' polymeric chains. Inorgani Chemistry Communication, 2013, 33, 99-104.	i C 3.9	11
83	Synthesis, structure, spectroscopic and ferroelectric properties of an acentric polyoxotungstate containing 1:2-type [Sm(l±-PW11O39)2]11â^' fragment and d-proline components. Spectrochimica Acta - Part A: Molecular and Biomolecular Spectroscopy, 2015, 134, 101-108.	3.9	11
84	Lanthanide-Incorporated Borotungstates Including Keggin-type [BW ₁₁ O ₃₉] ^{9–} Fragments and Their Luminescence Properties. Crystal Growth and Design, 2020, 20, 362-369.	3.0	11
85	Recent advances in isopolyoxotungstates and their derivatives. Acta Crystallographica Section C, Structural Chemistry, 2018, 74, 1202-1221.	0.5	11
86	Nicotinic-Acid-Ornamented Tetrameric Rare-Earth-Substituted Phospho(III)tungstates with the Coexistence of Mixed Keggin/Dawson Building Blocks and Its Honeycomb Nanofilm for Detecting Toxins. Inorganic Chemistry, 2021, 60, 14457-14466.	4.0	10
87	Syntheses, structures and properties of a series of inorganic–organic hybrid copper–lanthanide heterometal comprising germanotungstates with mixed ligands. Synthetic Metals, 2016, 217, 256-265.	3.9	9
88	Preparations, Structures and Luminescence Properties of Pentaâ€rareâ€earth Incorporated Tetravacant Dawson Selenotungstates and Their Ho ³⁺ /Tm ³⁺ Coâ€doped Derivatives. Chemistry - an Asian Journal, 2020, 15, 1156-1166.	3.3	9
89	A six-connected 3-D framework [enH2]2[Cu(en)2]3[H2W12O42]·6H2O constructed from paratungstate-based polyoxometalate units. Inorganic Chemistry Communication, 2012, 25, 35-38.	3.9	8
90	Hydrothermal synthesis and structural characterization of an organic–inorganic hybrid sandwich-type tungstoantimonate [Cu(en)2(H2O)]4[Cu(en)2(H2O)2][Cu2Na4(α-SbW9O33)2]·6H2O. Journal of Solid State Chemistry, 2014, 209, 113-119.	2.9	8

#	Article	IF	CITATIONS
91	Synthesis, structure and properties of an organic–inorganic hybrid independent 1-D double-chain Keggin-type silicotungstate with mixed ligands. Inorganic Chemistry Communication, 2015, 54, 25-30.	3.9	8
92	Three Types of Mixed Alkaliâ€Metalâ€, Transitionâ€Metalâ€, or Rareâ€Earthâ€Substituted Sandwichâ€Type Arsenotungstates with Supporting Rareâ€Earth Pendants. European Journal of Inorganic Chemistry, 2018, 2018, 143-152.	2.0	8
93	Syntheses, structures and properties of three new two-dimensional Cul–LnIII heterometallic coordination polymers based on 2,2′-dipyridyl-5,5′-dicarboxylate ligands. Spectrochimica Acta - Part A: Molecular and Biomolecular Spectroscopy, 2013, 116, 348-354.	3.9	7
94	Syntheses, structures and properties of three metal–organic complexes containing 2,2′-dipyridyl-5,5′-dicarboxylate ligands. Journal of Solid State Chemistry, 2015, 221, 5-13.	2.9	7
95	Synthesis, structure and electrochemical properties of an inorganic–organic hybrid Cu II Ce III heterometallic germanotungstate. Inorganic Chemistry Communication, 2016, 71, 54-60.	3.9	7
96	Hydrothermal syntheses, crystal structures and characterization of two new 1-D and 2-D inorganic–organic hybrid polyoxomolybdates [H 2 dap] 2 [x-Mo 8 O 26]·2H 2 O and [Cu(dap) 2] 2 [β-Mo 8 O 26]. Inorganic Chemistry Communication, 2016, 63, 24-29.	3.9	7
97	A trimeric tri-Tb ³⁺ including antimonotungstate and its Eu ³⁺ /Tb ³⁺ /Dy ³⁺ /Gd ³⁺ -codoped species with luminescence properties. Dalton Transactions, 2020, 49, 12401-12410.	3.3	7
98	Double Trigonal Pyramidal {SeO3} Groups Bridged 2-Picolinic Acid Modified Cerium-Inlaid Polyoxometalate Including Mixed Selenotungstate Subunits for Electrochemically Sensing Ochratoxin A. Inorganic Chemistry, 2022, 61, 1949-1960.	4.0	7
99	Organic–inorganic hybrid phosphite-participating S-shaped penta-Celll incorporated tellurotungstate as electrochemical enzymatic hydrogen peroxide for β-D-glucose detection. Inorganic Chemistry Frontiers, 0, , .	6.0	7
100	A Pentaâ€Eu ^{III} Sandwiched Dawson Selenotungstate and Its Unique Luminescence Properties. European Journal of Inorganic Chemistry, 2020, 2020, 3416-3425.	2.0	6
101	Two octamolybdate-based hybrids functionalized by 1,3-bis[tris(hydroxymethyl)methylamino]propane ligand. Inorganic Chemistry Communication, 2015, 61, 68-72.	3.9	5
102	Syntheses, structures and properties of two copper-2-picolinic-acid germanomolybdate hybrids with mixed organic components. Inorganic Chemistry Communication, 2016, 71, 113-118.	3.9	5
103	Syntheses, structural characterization and electrochemical properties of two rare-earth–isonicotinic-acid containing silicomolybdates. Inorganic Chemistry Communication, 2017, 83, 1-6.	3.9	5
104	A novel inorganic–organic hybrid 3d–4f heterometallic germanotungstate based on saturated Keggin-type [α-GeW12O40]4â^' polyanion. Inorganic Chemistry Communication, 2019, 108, 107542.	3.9	5
105	Two Innovative Fumaric Acid Bridging Lanthanide-Encapsulated Hexameric Selenotungstates Containing Mixed Building Units and Electrochemical Performance for Detecting Mycotoxin. Inorganic Chemistry, 2022, 61, 10965-10976.	4.0	5
106	A novel organic–inorganic hybrid 3D framework based on neodymium oxalate–selenites [Nd2(SeO3)2(C2O4)(H2O)2]·2H2O. Synthetic Metals, 2012, 162, 1648-1653.	3.9	4
107	Synthesis, characterization, magnetic and electrochemical properties of a new 3D hexa-copper-substituted germanotungstate. Journal of Solid State Chemistry, 2013, 205, 82-90.	2.9	4
108	A 3-D framework based on mono-copper II substituted silicotungstate units [Cu(dap) 2 (H 2 O)] 2 [Cu(dap) 2][α-SiW 11 CuO 39]·2H 2 O. Inorganic Chemistry Communication, 2014, 50, 19-23.	3.9	4

#	Article	IF	CITATIONS
109	Syntheses and Structures of Two Organic–Inorganic Composite Vanadoborates Na2(Hen)4[B18V12O60]·16H2O and (H2en)6[B18V12O60]2·2tepa·11H2O. Synthesis and Reactivity in Inorganic, Metal Organic, and Nano Metal Chemistry, 2016, 46, 687-693.	0.6	4
110	Hydroxyl-and-carboxyl ligand concatenating multi-lanthanide substituted tellurotungstates and electrochemical detection of noradrenaline. Journal of Rare Earths, 2022, 40, 1785-1793.	4.8	3
111	Syntheses, structural characterization and photoluminescence properties of {AsO 2 (OH)}-bridging arsenotungstates incorporating lanthanide ions. Journal of Solid State Chemistry, 2017, 256, 196-202.	2.9	2
112	A novel 1-D chain organic–inorganic hybrid Cull–PrIII heterometallic germanomolybdate decorated by 2-picolinic acid ligands. Inorganic Chemistry Communication, 2020, 113, 107764.	3.9	2
113	Synthesis, Structure, and Properties of a 2-D Organic–Inorganic Hybrid Phosphotungstate-Based Cu ^{II} –La ^{III} Heterometallic Derivative. Synthesis and Reactivity in Inorganic, Metal Organic, and Nano Metal Chemistry, 2014, 44, 171-176.	0.6	1
114	Synthesis, Crystal Structure, and Magnetic Property of an Organic–Inorganic Hybrid Silicotungstate With Supporting Dinuclear Copper Complexes. Synthesis and Reactivity in Inorganic, Metal Organic, and Nano Metal Chemistry, 2015, 45, 682-687.	0.6	1
115	Frontispiece: Aggregation of Giant Cerium–Bismuth Tungstate Clusters into a 3D Porous Framework with High Proton Conductivity. Angewandte Chemie - International Edition, 2018, 57, .	13.8	1
116	Two 1,3-bis[tris(hydroxymethyl)methylamino]propane functionalized 3d–4f heterometallic arsenotungstates. Inorganic Chemistry Communication, 2019, 105, 63-68.	3.9	1
117	A 1-D chain transition-metal substituted germanomolybdate constructed from di-Cull-substituted sandwich-type heteropolyoxomolybdate units linked by doubly di-Nal-cluster bridges. Inorganic Chemistry Communication, 2019, 99, 119-125.	3.9	1
118	A terbium-antimony-oxo-cluster bridging antimonotungstate comprising divacant and tetravacant Keggin segments. Inorganic Chemistry Communication, 2020, 111, 107625.	3.9	1
119	Alkali metal–lanthanide co-encapsulated 19-tungsto-2-selenate derivative and its electrochemical detection of uric acid. Inorganic Chemistry Communication, 2021, 130, 108734.	3.9	1
120	Hydrothermal Synthesis and Structural Characterization of a 1-D Inorganic-Organic Composite Tetra-Nickel Substituted Sandwich-Type Phosphotungstate. Synthesis and Reactivity in Inorganic, Metal Organic, and Nano Metal Chemistry, 2014, 44, 118-124.	0.6	0
121	Two Organic–Inorganic Hybrids Assembled from Transition–Metal Complexes and Keggin-Type Silicotungstates. Journal of Cluster Science, 2015, 26, 2005-2022.	3.3	0
122	Frontispiz: Aggregation of Giant Cerium–Bismuth Tungstate Clusters into a 3D Porous Framework with High Proton Conductivity. Angewandte Chemie, 2018, 130, .	2.0	0